Effects of elevated carbon dioxide on contraction force and proteome composition of sea urchin tube feet

Nopparat Nasuchon[1], Katsuya Hirasaka[2], Kenichi Yamaguchi[2], Jiro Okada[2] and Atsushi Ishimatsu[3]

[1] Graduate School of Fisheries and Environmental Sciences, Nagasaki University, 1551-7 Taira-machi, Nagasaki 851-2213, Japan and Chumphon Marine Fisheries Research and Development Center, Department of Fisheries, 408 M. 8, Paknam, Muang, Chumphon, Thailand, 86120, Email: bb53512001@ms.nagasaki-u.ac.jp

[2]Graduate School of Fisheries and Environmental Sciences, Nagasaki University, 1-14 Bunkyo, Nagasaki 852-8521, Japan, email: hirasaka@nagasaki-u.ac.jp; kenichi@nagasaki-u.ac.jp; jokada@nagasaki-u.ac.jp

[3] Institute for East China Sea Research, Nagasaki University, 1551-7 Taira-machi, Nagasaki 851-2213, Japan, email: a-ishima@nagasaki-u.ac.jp

Corresponding author: Nopparat Nasuchon

Tel: +81-95-850-7311,

Fax: +81-95-840-1881

Email: bb53512001@ms.nagasaki-u.ac.jp or inwiset2810@gmail.com

Abstract

This study examined how contraction force and protein profiles of the tube feet of the sea urchin (*Pseudocentrotus depressus*) were affected when acclimated to 400 (control), 2000 and 10000 μatm CO_2 for 48 days. Acclimation to higher CO_2 conditions significantly reduced contraction force of the tube feet. Two-dimensional gel electrophoresis showed that eight spots changed in protein volume: six up-regulated and two down-regulated. Using matrix-assisted laser desorption/ionization-quadrupole ion trap-time of flight mass spectrometry, three up-regulated spots (tubulin beta chain, tropomyosin fragment, and actin N-terminal fragment) and two down-regulated spots (actin C-terminal fragment and myosin light chain) were identified. One possible interpretation of the results is that elevated CO_2 weakened contraction of the tube feet muscle through an alteration of proteome composition, mainly associated with post-translational processing/proteolysis of muscle-related proteins.

Keywords: Sea urchins, Tube feet, Muscle contraction, Proteomics

1. Introduction

There are two processes by which seawater is acidified by the addition of carbon dioxide (CO_2), ocean acidification and accidental leakage from a carbon capture and storage (CCS) site. Ocean acidification occurs by absorption of CO_2 across sea surface from the atmosphere, and now widely recognized as a serious threat to the structure and function of marine ecosystems in the coming decades. Reductions in surface ocean pH by ocean acidification have been confirmed at a number of observation sites in the world oceans (Orr, 2011). It is estimated that approximately 30% of anthropogenic CO_2 emission has been absorbed by the ocean since 1960s (Le-Quéré et al., 2009). Dissolved CO_2 reacts with seawater to shift carbonate equilibria and thereby reduce seawater pH (Zeebe and Wolf-Gladrow, 2001). Average surface seawater pH is considered to have decreased by 0.1 units since the beginning of industrial revolution (Sabine et al., 2004) and is expected to decrease by further 0.8 units by 2300, when the atmospheric CO_2 concentration is projected to reach 1900 ppm (Caldeira and Wicket, 2003). The CCS technology has been developed to mitigate the effect of CO_2 related to the continued reliance on fossil fuels as prevalent energy source (IPCC, 2005). With CCS technology, CO_2 is separated from flue gas at large industrial and energy-related sources, transported to a storage site and injected into a geological formation, and hence isolated from the atmosphere for a long period of time (Schrag, 2009). Globally, there are 15 large-scale projects in operation, with a further seven under construction (Global CCS Institute, 2015). Accidental leakage of stored CO_2 through the seabed, which might impact benthic ecosystems near a leakage site, has been one of the major concerns with CCS technology (Taylor et al., 2014). The spatial extent of an acidification event will depend on the position of the CCS infrastructure and the nature of the leak. At the present time, we have little to no experience with CCS leakage, and therefore it is difficult to predict how and

to what extent marine faunas and floras near the leakage site would be affected. If CO_2 leakage occurs, CO_2 concentrations in the surrounding seawater can reach much higher levels than those predicted from ocean acidification. Therefore, the CO_2 levels used in the recent risk assessment studies of leakage from CCS sites are as high as 18325 µatm (Murray et al., 2013), 20000 µatm (Restelli et al., 2015), 29000 µatm (Ishida et al., 2013), or even up to 313862 µatm (De Orte et al., 2014), one or two orders of magnitude higher than in ocean acidification studies (typically up to 1000 or 2000 µatm).

Effects of CO_2 on marine organisms have become a focus of marine biological research during the past 20 years, mainly because of the increasing concern with the impacts of ocean acidification (Gattuso and Hansson, 2011) and potential CO_2 leakage from a CCS site (Noble et al., 2012) on marine ecosystem structures and ecological services. It is now generally accepted that calcification (i.e., the formation of $CaCO_3$ structures from Ca^{2+} absorbed from seawater and HCO_3^- generated by metabolism and originated from seawater carbon pool, Furla et al. 2000) is one of the most sensitive biological processes negatively affected by seawater acidification (Kroeker et al. 2013). For example, Li et al. (2016) recently demonstrated that the tubes of serpulid worm *Hydroides elegans* had lower hardness and a smaller radius when subjected to the projected acidic conditions for 2100 (pH 7.8), causing the worm to be mechanically weaker, although different organisms may show different sensitivities and response patterns (Ries et al. 2009). In addition, an increasing amount of data have become available on CO_2 effects on early development, growth, metabolism, photosynthesis, and survival of marine organisms (Kroeker et al. 2013). By comparison, very little is known on how CO_2 affects the integrity and functionality of muscular systems among marine animals. Wood et al. (2008) reported that the muscle mass in the arms of the brittlestar, *Amphiura filiformis*, decreased in lowered pH (7.7, 7.3 and 6.8) but

79 without structural changes in muscles, while in another species *Ophiura ophiura* muscle density
80 remained unaffected in lowered pH (7.7 and 7.3; PCO_2 1300–1400 and 2300–2500 μatm, Wood
81 et al. 2010). Schalkhausser et al. (2013) found significant declines in the force generated by the
82 adductor muscle in the king scallop, *Pecten maximanus*, collected in Norway and reared under
83 PCO_2 of 1120 μatm at 10°C. However, the effect was not detected in the same species from
84 France under the same experimental conditions (Schaulkhausser et al. 2014).
85 The purpose of this study was to examine the effect of CO_2 on contraction force and protein
86 composition of the tube feet of the sea urchin, *Pseudocentrotus depressus*. Tube feet are unique
87 hydraulic mechano-sensory adhesive organs found in echinoderms. Tube feet have a variety of
88 functions including light sensitivity, respiration, chemoreception and locomotion (Lesser et al.,
89 2011). They consist of a basal extensible cylinder, the stem, which bears an apical flattened disc
90 that makes contact with and adheres to the substratum. The stem wall of a tube foot consists of an
91 outer epidermis, a basiepidermal nerve plexus, a connective tissue layer (mutable collagenous
92 tissue), a myomesothelium (retractor muscle) and an inner epithelium that surrounds the water-
93 vascular lumen (Santos, 2005). Recent proteomic characterization of tube feet from the sea urchin
94 *Paracentrotus lividus* identified 328 non-redundant proteins, including 44 phospho-proteins and
95 18 glycoproteins, and revealed that the organs are composed of sensory-perception-related
96 proteins, nerve-related proteins, muscle-related proteins, development/regeneration-related
97 proteins, immunological-response-related proteins, and temporary-adhesion-related proteins
98 (Santos et al., 2013). While in-depth proteomics has been reported in sea urchin tube feet, a
99 comparative analysis of the tube feet proteomes in response to an environmental change, such as
100 ocean acidification, remains to be elucidated. We examined the contraction force and proteome
101 composition of tube feet under three CO_2 concentrations based on the present-day level (400

µatm), the prediction by IPCC in the year 2300 (2000 µatm) and extreme conditions (10000 µatm) predicted as the model of CCS leakage. Adult sea urchins (*P. depressus*) were acclimated to these CO_2 concentrations for 48 days. The contraction force was measured using isolated tube foot preparations. Proteomic analysis was applied to elucidate the response of muscle contraction to elevated CO_2 at the molecular level.

2. Materials and methods

2.1. Animal collection and maintenance

Wild adult sea urchins were collected by a local fisherman in Saga Prefecture, Japan (33°32'55.82" N; 129°50'56.74" E). Their shell diameter and wet body weight were 54.26 ± 2.26 mm and 56.12 ± 6.24 g (Mean ± SD, n = 42) respectively. The sea urchins were transferred to the Institute for East China Sea Research of Nagasaki University, Japan and stocked for 10 days in a 100 L tank supplied with a continuous flow of filtered seawater at 2 L/min at ambient pH (8.17) and temperature (23.3–24.0 °C). The sea urchins were fed with artificial food pellets prepared according to the recipe by Hiratsuka and Uehara (2007) every second day.

2.2. CO_2 exposure

The sea urchins were acclimated for 48 days (from 13 July to 27 August 2014) in seawater equilibrated with ambient air (400 ppm CO_2, seawater pH 8.2, control), or CO_2-enriched air at a concentration of 2000 ppm (pH 7.6, ocean acidification) or 10000 ppm (pH 7.0, CCS leakage). The sea urchins were reared individually in seven replicate containers (14×22×14 (depth) cm) per treatment placed in a water bath (120×75×20 (depth) cm) with a water depth of 12 cm.

Seawater was double filtered (150 µm and with string-wound cartridges) before being supplied to the header tanks. The filtered seawater was gravity-fed from the header tank to each of the 7 rearing containers at a flow rate of 50 mL/min. Seawater in the header tanks was bubbled continuously with an outside air at flow rate of 10 L/min for the control condition, or with CO_2-enriched air (2000 or 10000 ppm), which was prepared with a gas blender (Kofloc, GB-2C, Japan) by mixing dried air and pure CO_2 for the two higher CO_2 conditions. In addition, seawater in the rearing containers was gently bubbled with the same gases. The seawater temperature was kept stable at 25°C. The water baths were covered with plastic sheet to avoid CO_2 exchange with room air. Seawater pH (NBS) and dissolved oxygen concentration were monitored every second day with a digital multiparameter meter (WTW multi 3420, Germany) calibrated with a standard buffer solution of pH 4.01, 6.86 and 9.18. Salinity and temperature were monitored daily throughout the experiment using a salinity refractometer (S/Mill-E, Atago, Japan) and a solar digital thermometer (SN-1200, Netsuken, Japan). Alkalinity was measured weekly with a total alkalinity titrator (Kimoto, ATT-05, Japan). Partial pressure of CO_2 (PCO_2) was calculated from the data of seawater pH, temperature, salinity and alkalinity, using the CO2SYS program (E. Lewis, Brookhaven National laboratory).

2.3. Measurement of tube feet contraction

Seven sea urchins, one from each rearing container, were used per treatment for the measurement of the contraction force of isolated tube foot. A small piece (0.5 cm^2) of the lateral side of test was snipped off with the tube feet, submerged in seawater at room temperature with the same PCO_2 level as during acclimation, and continuously superfused with the seawater using a gravity-feeding apparatus. The cut end of the test and the tip of a tube foot were each pinched

using a pair of micro bulldog clamps. The clamp at the tip of the tube foot was connected to the probe of an isometric transducer (SB-1T, Nihon Kohden, Tokyo, Japan). The tube foot was gradually extended to a length of about 20-30 mm from its base, using a micromanipulator, until spontaneous rhythmic contractions occurred as seen in intact animals. To induce maximal contraction, the perfusate was switched from seawater to seawater containing 10^{-4} M acetylcholine (Ach) (Florey and Cahill, 1980), and the response was recorded until contraction force began to decrease. ACh is the natural excitatory transmitter substance in sea urchin tube feet (Florey et al., 1975). The maximal value was used as a contraction force in each measurement. The number of successful measurements in each animal varied from 1 to 3 (i.e., 1 to 3 tube feet because each tube foot was used only once), depending on the animal's physiological conditions. We used average values of each sea urchin for statistical comparison (Table S1).

2.4. Collection of tube feet for proteomic analysis

Four sea urchins were used per treatment for this purpose. Approximately 10 to 60 mg of tube feet were isolated on ice under a microscope from each sea urchin. To prevent protein digestion, the tube feet were soaked in 1 mL protease inhibitor solution (one tablet of cOmplete™ Mini/10 mL seawater, Roche, Indianapolis, IN, USA) during collection, and then placed into a 2-mL screw-cap centrifuge tube (Sarstedt, Nümbrecht, Germany). The samples were centrifuged at 12000×g for 1 min to remove the seawater. Subsequently, the samples were weighed and kept at –80°C until analysis.

2.5. Protein extraction

171 To accomplish extraction, separation and identification of proteins from a small amount of
172 tube feet, we applied a small-scale proteomic approach (Yamaguchi, 2011; Khandakar et al.,
173 2013)

174 One milliliter of Trizol reagent (Life Technologies, Carlsbad, CA, USA), 100 µg of zirconia
175 beads (0.6 mm in diameter, BMS, Tokyo, Japan), and a stainless-steel bead (5 mm in diameter,
176 BMS, Tokyo, Japan) were added to the frozen tube feet in a 2 mL screw-cap centrifuge tube
177 (Sarstedt, Nümbrecht, Germany). The tubes were mounted in a Master Rack aluminium block
178 (BMS, Tokyo, Japan) and agitated for 2 min at 25ºC in a ShakeMaster Auto ver 1.5 (BMS, Tokyo,
179 Japan). The homogenates were incubated at 25ºC for 5 min and 0.2 mL of chloroform was added
180 to each tube. The tubes were then shaken vigorously by hand for 15 s and incubated at 25ºC for 3
181 min. The mixture was centrifuged (12000×g, 15 min, at 4ºC) to separate it into a lower organic
182 phase, an interphase, and an upper aqueous phase. After removing the aqueous phase, 300 µL of
183 ethanol was added to the tube. The sample was mixed by inversion 3–5 times, incubated at 25ºC
184 for 3 min, and then centrifuged (12000×g, 1 min, at 4ºC) to remove the DNA pellets.

185 The resulting supernatant was transferred to dialysis tubing with a 3500 Da molecular weight
186 cut-off (Spectra/Por RC dialysis membrane 3, Spectrum Laboratories, Inc., Rancho Dominguez,
187 CA, USA), and dialyzed against 400 volumes of Milli-Q water (once renewed) for 72 h at 4ºC.
188 The dialysate was dehydrated with solvent-absorbent powder (Spectra/Gel Absorbent, Spectrum
189 Laboratories, Inc., Rancho Dominguez, CA, USA), suspended in 300 µL of IEF solution A
190 without carrier ampholite (8 M urea, 50 mM DTT, 2% w/v CHAPS, 0.001% w/v bromophenol
191 blue), incubated at 25ºC for 16 h, and centrifuged (15000×g, 15 min, 25ºC). The supernatant
192 was transferred to a new tube and the remaining pellet was re-suspended with 100 µL of IEF
193 solution A, centrifuged (15000×g, 15 min, 25ºC) and the supernatant was combined with the

first supernatant (total 400 µL). The combined supernatant (4 aliquots of 100 µL in a 0.5 mL Safe-Lock Protein LoBind Tube, Eppendorf, Hamburg, Germany) was stored at –70ºC. Protein concentration was determined using RC DC™ Protein Assay Kit (Bio-Rad, Hercules, CA, USA), with bovine serum albumin (BSA) as a standard.

2.6. Two-Dimensional gel electrophoresis (2-DE)

The first dimensional IEF separation was carried out using a 7-cm ReadyStrip® IPG Strips (Linear pH gradient, pH 3–10, Bio-Rad). The IPG strips were passively rehydrated for 12 h at room temperature in 125 µL of resuspension solution (8 M urea, 50 mM DTT, 2% w/v CHAPS, 0.2% carrier ampholytes, 0.0001% bromophenol blue), containing 30 µg protein/strip. IEF was carried out at 20°C, for a total of 20000 Vh (15 min with a 0–250 V linear gradient; 2 h with a 250–4000 V linear gradient; and finally 4000V held constant until 20000 Vh had been reached). After IEF, the IPG strips were incubated in 2.5 mL of 2% DDT-containing equilibration buffer (6 M urea, 2% SDS, 0.375 M Tris-HCl, pH 8.8, 20% glycerol) for 20 min and then incubated with 2.5% iodoacetamide-containing equilibration buffer for 20 min at room temperature. The second dimensional electrophoresis was performed with a Mini-PROTEAN Tetra electrophoresis cell (Bio-Rad, Hercules, CA, USA). The equilibrated IPG strips were placed on the top of a Mini-PROTEAN TGX® precast gels, sealed with ReadyPrep® overlay agarose (Bio-Rad) and electrophoresed at 200 V in running buffer (25 mM Tris base, 192 mM glycine and 0.1% w/v SDS), for 30 min at room temperature. Gels were fixed with a fixing solution (40% ethanol, 10% acetic acid) for 2 h. Following this, the gels were stained with Flamingo® fluorescent stain (Bio-Rad) and the gel images for figure presentation were captured using a GELSCAN® laser scanner (iMeasure, Nagano, Japan). For quantitative analysis of 2-DE patterns and spot volumes, a total

of 24 gel images, consisting of four biological replicates (i.e., proteins individually prepared from four specimens per treatment) and two technical replicates for each protein sample, were compared using the Prodigy SameSpots® software package (Non-linear Dynamics, Newcastle, UK). Reproducible gel spots were counted using the same software during spot alignment and pre-filtering stages.

2.7. Protein in-gel digestion and MALDI-QIT-TOF mass spectrometry

Protein spots were manually excised from the 2D gels using a spot image analyzer (FluoroPhoreStar 3000®, Anatech, Tokyo, Japan) equipped with a gel picker (1.8 mm in diameter). The methods we used for in-gel digestion and peptide extraction were slightly modified from the previously described methods of Shevchenko et al. (2006) and Khandakar et al. (2013). To reduce self-digestion of trypsin and avoid contamination, we used Trypsin Singles (proteomics grade, Sigma-Aldrich, MO, USA) at a lower concentration (10 ng/μL trypsin in 25 mM ammonium bicarbonate containing 10% acetonitrile) instead of Trypsin (sequencing grade, modified, Promega Corp. 13 ng/μL trypsin in 10 mM ammonium bicarbonate containing 10% acetonitrile) used by Shevchenko et al. (2006). Expecting faster peptide dryness, we used an extraction solution of 0.05% TFA in 50% acetonitrile, instead of 5% formic acid in 50% acetonitrile (Yamaguchi, 2011; Khandakar et al., 2013). In brief, the samples were dehydrated in 100 μL of acetonitrile and agitated for 10 min. The supernatant was withdrawn. The residues were added with 8 μL of the Trypsin Singles and left on ice for 20 min. After removal of an excess amount of the solution, the gels were incubated at 37°C overnight. Twenty μL of the extraction solution was added to the tube, incubated at 37°C in a shaker (100 r/min) for 15 min, and sonicated in a cup horn sonicator (Astrason Ultrasoinic Processor XL2020, Misoinix, at

output level 4) for 1 min. The solutions were transferred to a new 0.5-mL centrifuge tube and then centrifuged with a Speed Vac (SPD 131 DDA, Thermo Scientific) at 200 rpm and at 45°C for 15 min. The dried samples were dissolved in 5 µL of 0.5 mg/mL of 2,5-dihydroxybenzoic acid (DHBA, Shimadzu, Japan) in 33% acetonitrile, 0.1% trifluoroacetic acid. The 1 µL samples of the solution were spotted onto a µFocus MALDI target plate (Hudson Surface Technology, NJ, USA) and dried at room temperature. MS and MS/MS spectra were obtained using a MALDI-QIT-TOF mass spectrometer (AXIMA Resonance, Shimadzu, Kyoto, Japan). MS/MS ion search was performed using MASCOT® version 2.3 (Matrix Science, London, UK) against SwissProt 2014_07 (5456000 sequences; 194259968 residues) and EST Echinidae 2015_04 (851028 sequences; 212054698 residues) in our own MASCOT server. Search parameters used were: enzyme, trypsin; maximum missed cleavages, 2; fixed modification; carbamidomethyl (C); variable modifications, oxidation (HW and M); peptide mass tolerance, ± 0.3 Da; fragment mass tolerance, ± 0.2 Da; mass values, monoisotopic. Mascot score was assigned to identify protein with significance threshold at $p < 0.05$ as shown in figure S1.

2.8. Determination of *pI* and MW

Theoretical isoelectric point (*pI*) and sequence mass of precursor protein were calculated using ProtParam (http://www.expasy.ch/tools/protparam.html). Observed *pI* was calculated from the horizontal migration of the spot. Observed mass was estimated from the vertical migration of the spot by the method of Weber and Osborn (1969).

2.9. Statistical analysis

One sample t-test was applied to determine difference between measured and nominal PCO_2 values in each treatment. One-way ANOVA was applied to determine difference between group means and Tukey's HSD run to confirm group differences using PASW statistics 18. For 2-DE pattern analyses, four biological replicates for each condition and two technical replicates for each protein sample were compared between different CO_2 levels. Differences in spot volumes were statistically evaluated using ANOVA at $p < 0.05$, using Prodigy SameSpots® software package (Non-linear Dynamics, Newcastle, UK). Differentially accumulated proteins were defined as significant at fold ratios ≥ 1.4.

3. Results

3.1 Seawater chemistry

Daily seawater temperature fluctuated slightly as air temperature varied between 23.4–25.2°C. Throughout the experiment, salinity remained at 34–35 PSU and the dissolved oxygen saturation was always above 90 % (Table 1). Seawater pH varied slightly but remained relatively stable throughout the experiment (Fig. 1). The seawater pH, PCO_2, and HCO_3^- and CO_3^{2-} concentrations all differed significantly between treatments (one-way ANOVA, Table 1). Measured PCO_2 values were not significantly different from corresponding nominal values at 400 or 2000 µatm, whereas it was not the case at 10000 µatm (one-sample t-test, $t_{400\mu atm} = 0.035$, $P = 0.975$; $t_{2000\mu atm} = 2.039$, $P = 0.111$; $t_{10000\mu atm} = 3.548$, $P = 0.024$).

3.2. Tube feet contraction force

There was no difference in test diameters or body weights of the sea urchins between treatments (one-way ANOVA, $F_{2,18} = 1.127$; $P = 0.346$ and $F_{2,18} = 0.475$, $P = 0.63$, respectively). Tube feet contraction force was significantly lowered with increasing CO_2 levels in a PCO_2-dependent manner (one-way ANOVA, $F_{2,18} = 13.89$, $P = 0.000$; Fig. 2). Multiple comparison analysis revealed that contraction force differed significantly between all pH treatments (Tukey's HSD, $P < 0.05$; Table S1).

3.3. Protein profile under changing in CO_2 concentration

The total protein amounts soluble to CHAPS-based IEF solution obtained from the tube feet in 400 µatm, 2000 µatm and 10000 µatm treatments were 0.65 ± 0.27, 1.60 ± 0.48 and 1.40 ± 0.33 mg g^{-1} fresh weight, respectively. The number of protein spots that were resolved from protein extracts from 400 µatm, 2000 µatm and 10000 µatm treatments were 120 ± 2, 120 ± 2 and 119 ± 1 respectively (Fig. 3. Comparative quantitative image analysis of 2-DE patterns showed that a total of eight protein spots changed significantly in spot volume (i.e. spot intensity); two spots were down-regulated and six spots were up-regulated under increasing CO_2 conditions (Figs. 3 and S1). Eight differentially accumulated protein spots (spots 1–8) and four constantly expressed protein spots (spots a-d, prominent spots selected for easier protein extraction/identification) were excised from the 2-DE gels (Figs. 3 and S1), digested in-gel with trypsin, and the extracted tryptic peptides were subjected to MALDI-QIT-TOF mass spectrometry. Although nucleotide/protein sequences reported from *Pseudocentrotus depressus* number less than one thousand (56 proteins and 941 ESTs), 9 of the 12 protein spots were positively identified by cross-species searches (Tables 2 and S2). Four constantly expressed proteins were identified as actin-1 (spot a), tropomyosin (spot b), voltage dependent anion channel 2 (spot c), and

calmodulin-A (spot d). Of the 6 up-regulated proteins, three were identified as tubulin beta chain (spot 2), tropomyosin (spot 3) and actin (spot 4). The other three (spots 1, 5, and 6) were not identified. Two down-regulated proteins were identified as myosin light chain (spot 7) and actin (spot 8). The observed masses of actins, spots 4 (25.4 kDa) and 8 (17.4 kDa), were significantly lower than the theoretical masses of actin (41.8 kDa) (Table 2). In contrast, the observed mass of constantly expressed actin (spot a, 39.0 kDa) is close to the theoretical mass. These observations and the peptides assigned to the actin sequence by MS/MS ions searches indicated that spots 4 and 8 were N-terminal and C-terminal fragments of actin, respectively (Tables 2 and S2). In a similar way, spot b (34.7 kDa) was considered to be intact tropomyosin, and spot 3 (28.3 kDa) a fragment of tropomyosin (Table 2).

4. Discussion

This study demonstrated that the contraction force of the tube feet was significantly reduced by 48 day exposure to 2000 and 10000 μatm CO_2 in the sea urchin, *P. depressus*. The mechanisms underlying this functional impairment are yet to be elucidated, but our proteomic analysis demonstrated alterations of proteome composition, mainly a consequence of post-translational processing and/or proteolysis of muscle-related proteins, which could give a clue for a mechanistic understanding of the physiological disorder. Presently, very little is known about the effects of ocean acidification and CO_2 leakage from CCS sites on muscular systems of marine invertebrates (see Introduction). We recently showed that CO_2 significantly reduced the locomotion speed of the sea urchin, *Hemicentrotus pulcherrimus*, reared under 1000 μatm PCO_2 both at ambient and at an elevated temperature (+ 2°C) for seven months (Yin, Lee, Kurihara and Ishimatsu, in preparation). Similarly, some studies showed negative impacts on muscle systems

in fish. Chambers et al. (2014) and Frommel et al. (2016) showed subtle histological alterations in skeletal muscle of the fish larvae (*Paralichthys dentatus* and *Thunnus albacares*) under elevated CO_2 conditions (1800 and 4700 μatm, and 2000–9600 μatm, respectively). Bignami et al. (2014) reported that maximum swimming velocity was reduced in pelagic larvae of *Coryphaena hippurus*, reared under 1460 μatm PCO_2 for 21 days, but this effect was absent in larvae of another pelagic fish, *Rachycentron canadum* (Bignami et al. 2013) reared under 2100 μatm for 22 days. On the other hand, there are studies demonstrating that fish were relatively insensitive to elevated CO_2. Maneja et al. (2013) found swimming activity of larval Atlantic cod, *Gadus morhua*, was robust to high CO_2 exposure, and Melzner et al. (2009) also found that critical swimming speed of adult *G. morhua* was unaffected by exposure to 5800 μatm PCO_2 for 12 months or 3100 μatm PCO_2 for 4 months. Furthermore, we have recently published the data on the effect of CO_2 and temperature on the escape response of the Japanese anchovy, *Engraulis japonicus* to mechanical stimuli, and found no significant difference in various parameters of the response except turning rate which was elevated at a higher temperature (Nasuchon et al. 2016).

One possible interpretation of the observed negative effects of CO_2 on locomotive behaviors in marine invertebrates (and fish) is that elevated CO_2 or resultant acidification of body fluids had direct negative impacts on the integrity and/or functionality of muscular system in these animals, as suggested by our proteome analysis. However, different hypotheses are also possible. Recent papers on the effect of ocean acidification on fish have demonstrated that increasing CO_2 can disrupt sensory and brain functions of fish (Nagelkerken and Munday, 2016). There is some evidence for the involvement of a neurotransmitter, gamma-aminobutyric acid (GABA) in these phenomena in fish under elevated CO_2 (Nilsson et al., 2012; Chivers et al., 2014; Hamilton et al., 2014). The current hypothesis for the involvement of GABA assumes decreased chloride ion

353 concentrations in extracellular fluid, as a result of acid-base restoration through ionic exchange
354 with bicarbonate ions, to be responsible for the reversed (from inhibitory to excitatory) response
355 to GABA released from a nerve terminal, as known under some pathological conditions (Nilsson
356 et al., 2012). GABA was detected in tube foot extract of sea urchins, and known to cause
357 excitation of cholinergic motoneurones but have no direct effect on muscle fibers (Florey et al.,
358 1975). However, since ion concentrations of perfusate were held constant during the
359 measurement, the reduced contraction force of the tube feet seen in this study was more likely
360 attributable to the effect of pH/CO_2 per se, rather than through some GABA-related process
361 triggered by lowered chloride concentrations. Sea urchins have a lower capacity for acid-base
362 regulation of both extracellular (Spicer et al., 2011; Stumpp et al., 2012; Kurihara et al., 2013)
363 and intracellular fluids (Stumpp et al., 2012) than fish (Ishimatsu et al., 2005), it is unlikely that
364 elevated CO_2 levels, at least those predicted in the context of ocean acidification, will cause
365 substantial decreases of chloride ion concentrations in the body fluids of intact sea urchins.
366 Another possibility is that 48-day exposure to CO_2 resulted in some irreversible alterations in the
367 functions of GABA receptors. Further, low pH per se could have reduced neuromuscular
368 transmission (Landau and Nachchen, 1975; Takahashi and Copenhagen, 1996). Clearly, further
369 studies are needed for mechanistic understanding of the observed reduction in the contraction
370 force of tube feet under elevated CO_2 conditions.

371 Our comparative quantitative analysis of 2-DE profiles detected eight protein spots that had
372 changed in spot volume. Of six up-regulated spots, three were identified as tubulin beta chain,
373 tropomyosin fragment and actin N-terminal fragment, while two down-regulated ones were
374 identified as myosin light chain and actin C-terminal fragment (see Results). These proteins are
375 all involved in muscle contraction. An interaction between actin and myosin generates movement

relative to each other. Troponin and tropomyosin are involved in regulating actin site (Szent-Györgyi, 1975). Myosin light chain of 17 kDa is an essential light chain (ELC), which has the role of stabilizing the lever arm. The interaction between the C-terminal of ELC of the domain and N-terminal sub-domain of the heavy chain of the myosin may be involved in coupling ATP hydrolysis and rotation of the lever arm (Ushakov, 2009). Our data showed that the majority of actin was constantly expressed as the intact protein under all the CO_2 conditions tested, whereas minor fragments of actin were differentially expressed: the actin C-terminal fragment decreased, while the actin N-terminal fragment increased at higher CO_2 levels. Actin has been shown to be cleaved by caspases into N-terminal 32-kDa (Fractin) and 15-kDa (tActin) fragments. The site of this proteolytic cleavage at the C-terminal side of ^{240}**YELPD**^{244} is conserved from yeast to humans, implicating it as an important regulatory sequence (Gourley and Ayscough, 2005). However, N- and C-terminal fragments of actin identified in this study contained the uncleaved sequence S**YELPD**GQVITIGNER (Figs S1 and S2), indicating the possibility that the accumulation of the actin N-terminal fragment in this study may have been a product of caspase-independent proteolysis of intact actin under elevated CO_2. A comparative proteomic analysis of the oyster *Crassostrea gigas* found up-regulated two isoform gene products of tropomyosin (33.06 kDa, *pI* = 4.57, and 26.91 kDa, *pI* = 4.49) in mantle tissue at 2000 µatm CO_2 (Wei et al 2015). In contrast, our study showed that the majority of tropomyosin was constantly expressed, while up-regulation was found in a short form (Table 2), derived from the same tropomyosin gene. Thus, the increased short form, most likely a fragment, of tropomyosin may also have affected muscle contraction. Voltage dependent anion channel 2 (VDAC2, spot c) and calmodulin-A (spot d) were identified as unchanged abundant proteins (Fig. 3 and Table 2). Unlike actin or tropomyosin, neither fragment of VDAC2 nor calmodulin-A was detected.

Therefore, these proteins were probably not responsible for the reductions in muscle contraction force at high CO_2 conditions in our sea urchins.

5. Conclusion and future study

We have shown that elevated CO_2 reduced the contraction force of sea urchin tube feet in a concentration-dependent manner. Further, 2-DE based proteomics showed that proteins involved in muscle contraction changed their spot volumes under high CO_2 conditions. These results suggest that elevated CO_2 possibly affects muscular system in sea urchins through alterations in proteome composition via a post-translational proteolysis, although other interpretations are also possible. For example, disruption of neuromuscular transmission or coordination at higher neuronal levels by elevated CO_2 or lowered pH in marine animals is a possibility. On the other hand, although this study pointed out the importance of proteomic approaches to understand how sea urchin tube feet respond to elevated CO_2 in the molecular level, correlation between transcriptomic and proteomic changes in response to elevated CO_2 remain to be elucidated. In addition, the muscular systems in various organs of sea urchins and other marine invertebrates need to be examined for their CO_2 sensitivity to understand how future oceanic environmental changes will affect physiological functions driven by muscle contraction.

Acknowledgement

We thank Prof. Tatsuya Oda and his laboratory members for their helpful advices and cooperation on small-scale proteomics. We also thank Mr. Shouhei Noma, Mr. Ryosuke Ono and Mr. Mail Văn Hiều for their assistance in samples preparation. Thanks are also due to Ms. Mizuri Murata and Ms. Takako Aketagawa for their help in collecting sea urchins. This study was

422 supported by Grant-in-Aid for Scientific Research by Japan Society for the Promotion of Science
423 (26281010).
424

425 **References**

426 Bignami, S., Sponaugle, S., Cowen, R.K., 2013. Response to ocean acidification in larvae of a
427 large tropical marine fish, *Rachycentron canadum*. Glob. Change Biol. 19, 996-1006.
428 Bignami, S., Sponaugle, S., Cowen, R.K., 2014. Effects of ocean acidification on the larvae of a
429 high-value pelagic fisheries species, mahi-mahi *Coryphaena hippurus*. Aquat. Biol. 21, 249-
430 260
431 Caldeira, K., Wickett, M.E., 2003. Oceanography: anthropogenic carbon and ocean pH. Nature
432 425, 365. doi:10.1038/425365a
433 Chambers, R.C., Candelmo, A.C., Habeck, E.A., Poach, M.E., Wieczorek, D., Cooper, K.R.,
434 Greenfield, C.E., Phelan, B.A., 2014. Effects of elevated CO_2 in the early life stages of
435 summer flounder,Paralichthys dentatus, and potential consequences of ocean acidification.
436 Biogeosciences 11, 1613–1626. doi:10.5194/bg-11-1613-2014
437 Chivers, D.P., McCormick, M.I., Nilsson, G.E., Munday, P.L., Watson, S-A., Meekan, M.G.,
438 Mitchell, M.D., Corkill, K.C., Ferrari, M.C., 2014. Impaired learning of predators and lower
439 prey survival under elevated CO_2: a consequence of neurotransmitter interference. Glob.
440 Change. Biol. 20, 515-522
441 De Orte, M.R., Sarmiento, A.M., DelValls, T.Á., Riba, I., 2014. Simulation of the potential effects
442 of CO_2 leakage from carbon capture and storage activities on the mobilization and speciation
443 of metals. Mar. Pollut. Bull. 86, 59–67. doi:10.1016/j.marpolbul.2014.07.042

444 Florey, E., Cahill, M.A., Rathmayer, M., 1975. Excitatory actions of AGBA and of acetylcholine
445 in sea urchin tube feet. Comp. Biochem. Physiol. 51C, 5–12.
446 Florey, E., Cahill, M. a, 1980. Cholinergic motor control of sea urchin tube feet: evidence for
447 chemical transmission without synapses. J. Exp. Biol. 88, 281–92.
448 Frommel, A.Y., Margulies, D., Wexler, J.B., Stein, M.S., Scholey, V.P., Williamson, J.E.,
449 Bromhead, D., Nicol, S., Havenhand, J., 2016. Ocean acidification has lethal and sub-lethal
450 effects on larval development of yellowfin tuna, *Thunnus albacares*. J. Exp. Mar. Bio. Ecol.
451 482, 18–24. doi:10.1016/j.jembe.2016.04.008
452 Furla, P., Galgani, I., Durand, I., Allemand, D., 2000. Sources and mechanisms of inorganic
453 carbon transport for coral calcification and photosynthesis. J. Exp. Biol. 203, 3445–3457.
454 Gattuso, J.P., Haussan L., 2011. Ocean acidification. Oxford University press, Oxford. 326 pp.
455 Global CCS Institute, 2015. The global status of CCS 2015: Summary report. Melbourne.
456 Gourlay, C.W., Ayscough, K.R., 2005. The actin cytoskeleton: a key regulator of apoptosis and
457 ageing? Nat. Rev. Mol. Cell Biol. 6, 583–589. doi:10.1038/nrm1682
458 Hamilton, T.J., Holcombe, A., Tresguerres, M., 2014. CO_2-induced ocean acidification increases
459 anxiety in Rockfish via alteration of GABAA receptor functioning. Proc. R. Soc. B.
460 doi:10.1098/rspb.2013.2509
461 Hiratsuka, Y., Uehara, T., 2007. Feeding Ecology of Four Species of Sea Urchins (Genus
462 Echinometra) in Okinawa 81, 85–100.
463 Ishida, H., Golmen, L.G., West, J., Krüger, M., Coombs, P., Berge, J.A., Fukuhara, T., Magi, M.,
464 Kita, J., 2013. Effects of CO_2 on benthic biota: An in situ benthic chamber experiment in
465 Storfjorden (Norway). Mar. Pollut. Bull. 73, 443–451. doi:10.1016/j.marpolbul.2013.02.009

Ishimatsu, A., Hayashi, M., Lee, K.S., Kikkawa, T., Kita, J., 2005. Physiological effects on fishes in a high-CO_2 world. J. Geophys. Res. C. Ocean. 110, C09S09.

IPCC, 2005. IPCC Special Report on Carbon Dioxide Capture and Storage. Cambridge University Press. 442 pp.

Khandakar, J., Haraguchi, I., Yamaguchi, K., Kitamura, Y., 2013. A small-scale proteomic approach reveals a survival strategy , including a reduction in alkaloid biosynthesis , in *Hyoscyamus albus* roots subjected to iron deficiency. Front. Plant. Sci. 4, 1–13. doi:10.3389/fpls.2013.00331

Kroeker, K.J., Kordas, R.L., Crim, R., Hendriks, I.E., Ramajo, L., Singh, G.S., Duarte, C.M., Gattuso, J.P., 2013. Impacts of ocean acidification on marine organisms: Quantifying sensitivities and interaction with warming. Glob. Chang. Biol. 19, 1884–1896.

Kurihara, H., Yin, R., Nishihara, G., Soyano, K., Ishimatsu, A., 2013. Effect of ocean acidification on growth, gonad development and physiology of the sea urchin *Hemicentrotus pulcherrimus*. Aquat. Biol. 18, 281–292. doi:10.3354/ab00510

Landau, E.M., Nachshen, D.A., 1975 The interaction of pH and divalent cations at the neuromuscular junction. J. Phyiol. 241, 775-790.

Le-Quéré, C., Raupach, M.R., Canadell, J.G., Al., G.M., 2009. Trends in the sources and sinks of carbon dioxide. Nat. Geosci. 2, 831 – 836.

Lesser, M.P., Carleton, K.L., Böttger, S.A., Barry, T.M., Walker, C.W., 2011. Sea urchin tube feet are photosensory organs that express a rhabdomeric-like opsin and PAX6. Proc. Biol. Sci. 278, 3371–9. doi:10.1098/rspb.2011.0336

Li, C., Menga, Y., Heb, C., Chanc, V.B.S., Yaob, H., and Thiyagarajan V. 2016. Mechanical robustness of the calcareous tubeworm Hydroides elegans: warming mitigates the adverse effects of ocean acidification. Biofouling 2, 191-204.

Maneja, R.H., Frommel, A.Y., Browman, H.I., Clemmesen, C., Geffen, A.J., Folkvord, A., Piatkowski, U., Durif, C.M.F., Bjelland, R., Skiftesvik, A.B., 2013. The swimming kinematics of larval Atlantic cod, Gadus morhua L., are resilient to elevated seawater pCO_2. Mar. Biol. 160, 1963–1972. doi:10.1007/s00227-012-2054-y

Melzner, F., Göbel, S., Langenbuch, M., Gutowska, M. a., Pörtner, H.O., Lucassen, M., 2009. Swimming performance in Atlantic Cod (*Gadus morhua*) following long-term (4-12 months) acclimation to elevated seawater PC O_2. Aquat. Toxicol. 92, 30–37. doi:10.1016/j.aquatox.2008.12.011

Murray, F., Widdicombe, S., McNeill, C.L., Solan, M., 2013. Consequences of a simulated rapid ocean acidification event for benthic ecosystem processes and functions. Mar. Pollut. Bull. 73, 435–442. doi:10.1016/j.marpolbul.2012.11.023

Nagelkerken I, Munday PL (2016) Animal behaviour shapes the ecological effects of ocean acidification and warming: moving from individual to community-level responses. Glob. Chang. Biol., 22, 974-989

Nasuchon, N., Yagi, M., Kawabata, Y., Gao, K., Ishimatsu, A., 2016. Escape responses of the Japanese anchovy *Engraulis japonicus* under elevated temperature and CO_2 conditions. Fish. Sci. 82, 435–444. doi:10.1007/s12562-016-0974-z

Nilsson, G.E., Dixson, D.L., Domenici, P., McCormick, M.I., Sørensen, C., Watson, S-A., Munday, P.L., 2012. Near-future carbon dioxide levels alter fish behaviour by interfering with neurotransmitter function. Nature. Clim. Change. 2, 201–204

510 Noble, R.R.P., Stalker, L., Wakelin, S.A., Pejcic, B., Leybourne, M.I., Hortle, A.L., Michael, K.,
511 2012. Biological monitoring for carbon capture and storage - A review and potential future
512 developments. Int. J. Greenh. Gas Control 10, 520–535. doi:10.1016/j.ijggc.2012.07.022
513 Orr, J.C., 2011. Recent and future changes in ocean carbonate chemistry. In: Gattuso J-P, Hansson
514 L (eds). Ocean acidification. Oxford University Press, Oxford.
515 Rastelli, E., Corinaldesi C., Dell'Anno A., Amaro T., Queirós, A.M., Widdicombe S., Danovaro
516 R., 2015. Impact of CO_2 leakage from sub-seabed carbon dioxide capture and storage (CCS)
517 reservoirs on benthic virus-prokaryote interactions and functions. Front Microbiol 6, 1–10.
518 doi:10.3389/fmicb.2015.00935
519 Ries, J.B., Cohen, A.L., McCorkle, D.C., 2009. Marine calcifiers exhibit mixed responses to
520 CO_2-induced ocean acidification. Geology 37, 1131–1134. doi:10.1130/G30210A.1
521 Sabine, C.L., Feely, R.A., Gruber, N., Key,R.M., Lee, K., Bullister, J.L., Wanninkhof, R., Wong,
522 C.S., Wallace, D.W.R., Tilbrook, B., Millero, F.J., Peng, T.H., Kozyr, A., Ono, T., Rios, A.S.,
523 2004. The oceanic sink for anthropogenic CO_2. Science 305, 367-371.
524 doi:10.1126/science.1097403
525 Santos, R., 2005. Adhesion of echinoderm tube feet to rough surfaces. J. Exp. Biol. 208, 2555–
526 2567. doi:10.1242/jeb.01683
527 Santos, R., Barreto, A., Franco, C., Coelho, A.V., 2013. Mapping sea urchins tube feet proteome-
528 -a unique hydraulic mechano-sensory adhesive organ. J. Proteomics 79, 100–13.
529 doi:10.1016/j.jprot.2012.12.004
530 Schalkhausser, B., Bock, C., Stemmer, K., Brey, T., Pürtner, H.O., Lannig, G., 2013. Impact of
531 ocean acidification on escape performance of the king scallop, *Pecten maximus*, from
532 Norway. Mar. Biol. 160, 1995–2006. doi:10.1007/s00227-012-2057-8

Schalkhausser, B., Bock, C., Pürtner, H.O., Lannig, G., 2014. Escape performance of temperate king scallop, *Pecten maximus* under ocean warming and acidification. Mar. Biol. 161, 2819–2829. doi:10.1007/s00227-014-2548-x

Schrag, D.P., 2009. Storage of carbon dioxide in off shore sediments. Science 325, 1658-1659.

Shevchenko, A., Tomas, H., Havlis, J., Olsen, J. V, Mann, M., 2006. In-gel digestion for mass spectrometric characterization of proteins and proteomes. Nat. Protoc. 1, 2856–2860. doi:10.1038/nprot.2006.468

Spicer, J.I., Widdicombe, S., Needham, H.R., Berge, J.A., 2011. Impact of CO_2-acidified seawater on the extracellular acid–base balance of the northern sea urchin *Strongylocentrotus dröebachiensis*. J. Exp. Mar. Bio. Ecol. 407, 19–25. doi:10.1016/j.jembe.2011.07.003

Stumpp, M., Hu, M.Y., Melzner, F., Gutowska, M.A., Dorey, N., Himmerkus, N., Holtmann, W.C., Dupont, S.T., Thorndyke, M.C., Bleich, M., 2012. Acidified seawater impacts sea urchin larvae pH regulatory systems relevant for calcification. Proc. Natl. Acad. Sci. U. S. A. 109, 18192–7. doi:10.1073/pnas.1209174109

Szent-Györgyi, A.G., 1975. Calcium regulation of muscle contraction. Biophys. J. 15, 707–23. doi:10.1016/S0006-3495(75)85849-8

Takahashi, K-I., Copenhagen, D.R., 1996 Modulation of neuronal function by intracellular pH. Neurosci. Res. 24, 109-116.

Taylor, P., Stahl, H., Vardy, M.E., Bull, J.M., Akhurst, M., Hauton, C., James, R.H., Lichtschlag, A., Long, D., Aleynik, D., Toberman, M., Naylor, M., Connelly, D., Smith, D., Sayer, M.D.J., Widdicombe, S., Wright, I.C., Blackford, J., 2014. A novel sub-seabed CO_2 release experiment informing monitoring and impact assessment for geological carbon storage. Int. J. Greenh. Gas Control 38, 3–17. doi:10.1016/j.ijggc.2014.09.007

556 Ushakov, D.S., 2009. Structure and function of the essential light chain of myosin. Biophysics
557 (Oxf). 53, 505–509. doi:10.1134/S0006350908060067
558 Weber, K., and Osborn, M., 1969. The reliability of molecular weight determinations by dodecyl
559 sulfate-polyacrylamide gel electrophoresis. J. Biol. Chem. 244, 4406–4412.
560 Wei, L., Wang, Q., Ning, X., Mu, C., Wang, C., Cao, R., Wu, H., Cong, M., Li, F., Ji, C., Zhao, J.,
561 2015. Combined metabolome and proteome analysis of the mantle tissue from Pacific oyster
562 *Crassostrea gigas* exposed to elevated pCO_2. Comp. Biochem. Physiol. Part D. Genomics
563 Proteomics 13, 16–23. doi:10.1016/j.cbd.2014.12.001
564 Wood, H.L., Spicer, J.I., Widdicombe, S., 2008. Ocean acidification may increase calcification
565 rates, but at a cost. Proc. R. Soc. B Biol. Sci. 275, 1767–1773. doi:10.1098/rspb.2008.0343
566 Wood, H.L., Spicer, J.I., Lowe, D.M., Widdicombe, S., 2010. Interaction of ocean acidification
567 and temperature; the high cost of survival in the brittlestar *Ophiura ophiura.* Mar. Biol. 157,
568 2001–2013. doi:10.1007/s00227-010-1469-6
569 Yamaguchi, K., 2011. Preparation and proteomic analysis of chloroplast ribosomes. Methods
570 Mol. Biol. 775, 241–264.
571 Zeebe, R.E., Wolf-Gladrow, D., 2001. CO_2 in seawater: equilibrium, kinetics, isotopes. Elsevier,
572 Amsterdam. 346 pp.
573
574
575
576
577
578

579

580

581

582

583

584

585

586

587

588

589

590

591

592

593

594

595

596

597

598

Fig. 1 Temporal changes in seawater pH during 48-day exposure experiment. Filled triangles represent 400 µatm, filled circles 2000 µatm, and filled squares 10000 µatm treatments.

Fig. 2 Contraction force (Newton, N) of the isolated tube feet of *Pseudocentrotus depressus* induced by 10^{-4} M acetylcholine (Mean ± SE, number of individuals = 7/treatment). The sea urchins were acclimated to 400 µatm (control), 2000 µatm and 10000 µatm PCO_2 for 48 days at 25°C. *Significant difference from 400 µatm, †significant difference from 2000 µatm (ANOVA $F_{2,18} = 13.89$, $P = 0.000$; Tukey's HSD, $P < 0.05$).

Fig. 3 Two-dimensional gel electrophoretic separations. Thirty µg of tube feet proteins extracted from *Pseudocentrotus depressus* treated in **A** 400 µatm, **B** 2000 µatm and **C** 10000 µatm were separated on 7-cm IPG strips. The first dimensional isoelectric focusing of 2-DE was performed using a pH range of 3-10. The characters a-d represent the constantly expressed proteins and the numbers 1-8 represent the differentially accumulated proteins.

Fig. 1

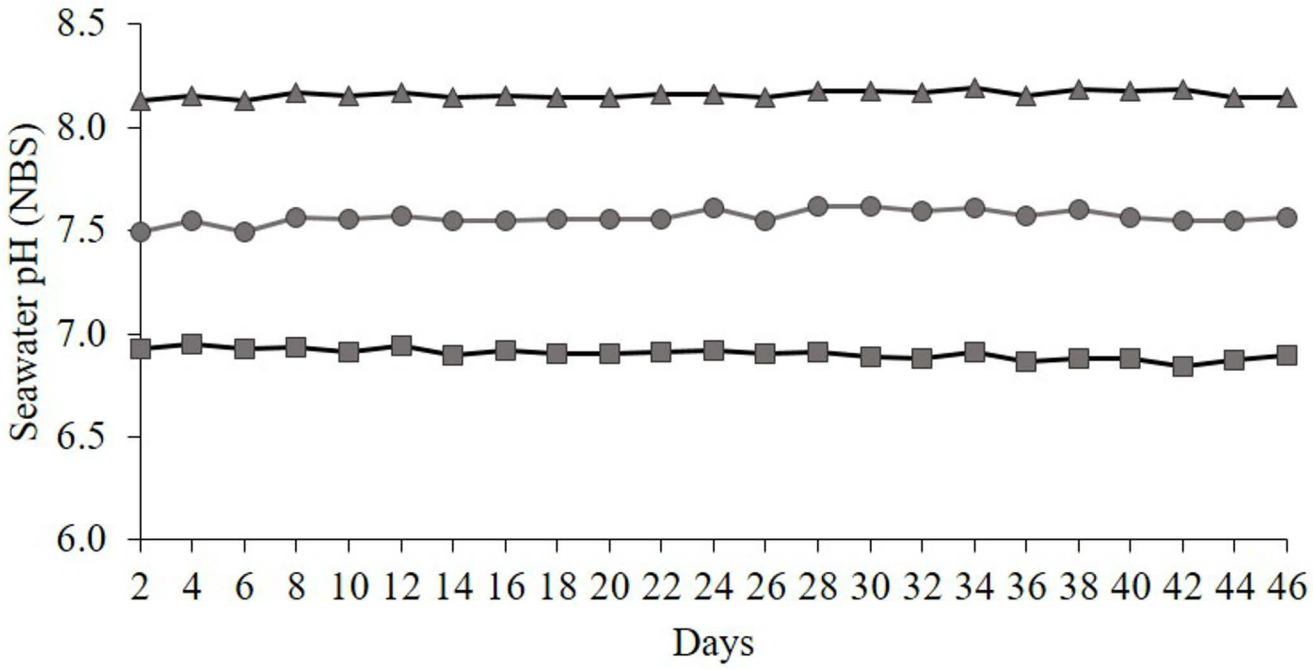
Seawater pH (NBS)
8.5
8.0
7.5
7.0
6.5
6.0
2 4 6 8 10 12 14 16 18 20 22 24 26 28 30 32 34 36 38 40 42 44 46
Days

Fig. 2

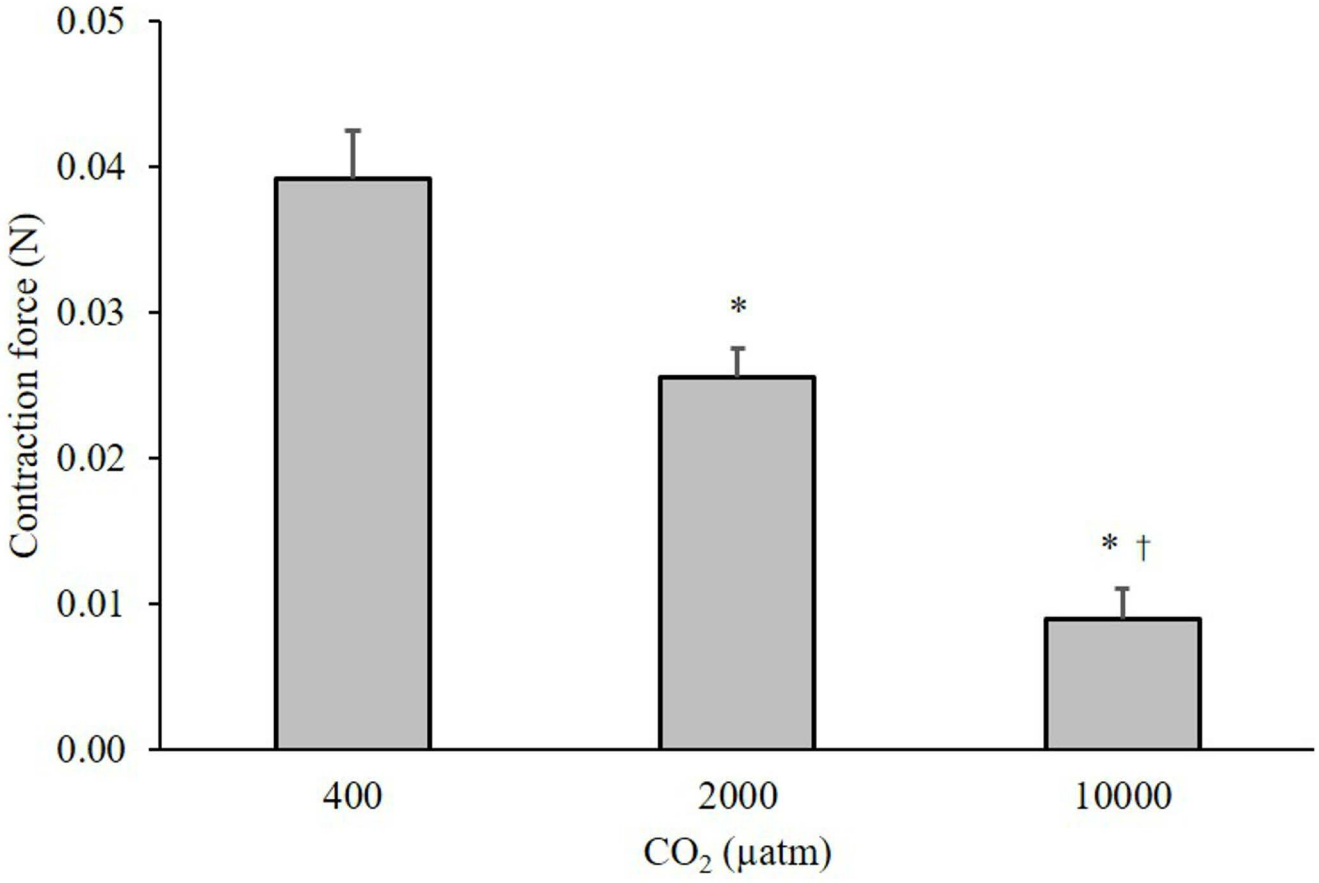
0.05
0.04
0.03
0.02
0.01
0.00
Contraction force (N)
*
* †
400
2000
10000
CO2 (µatm)

Fig. 3

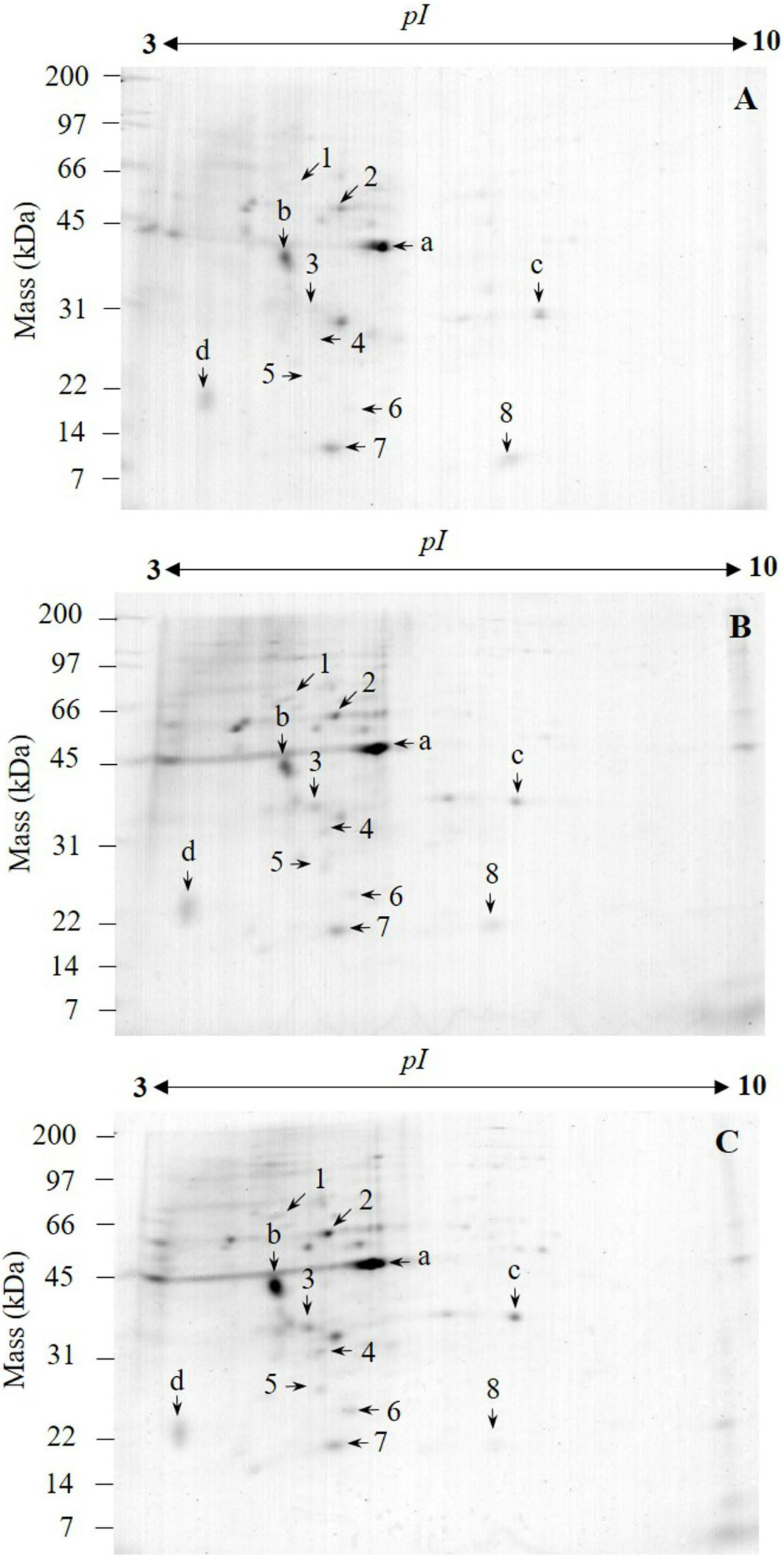

Table 1 Seawater pH, percentage dissolved oxygen (DO) saturation, temperature (Temp.), salinity, alkalinity (TA), partial pressure of carbon dioxide (PCO_2), bicarbonate (HCO_3^-) and carbonate (CO_3^{2-}) concentrations (mean ± SD) of each treatment

Treatment	400 (µatm)	2000 (µatm)	10000 (µatm)
$pH_{(NBS)}$	8.16 ± 0.02	7.56 ± 0.03[a]	6.90 ± 0.03[a,b]
DO (%)	96 ± 2	96 ± 2	96 ± 2
Temp. (°C)	24.6 ± 0.6	24.6 ± 0.6	24.6 ± 0.6
Salinity (PSU)	34.6 ± 0.6	34.6 ± 0.6	34.6 ± 0.6
TA (µmol/Kg-SW)	2121.3 ± 8.4	2128.1 ± 6.7	2130.2 ± 15.0
[1]PCO_2 (µatm)	400 ± 22	1912 ± 116	9307 ± 524*,†
[1]HCO_3^- (µmol/Kg-SW)	1677.7 ± 10.9	2009.0 ± 13.4*	2128.6 ± 12.4*,†
[1]CO_3^{2-} (µmol/Kg-SW)	196.8 ± 1.2	61.5 ± 3.5[a]	14.2 ± 0.7[a,b]

[1]Calculated from seawater pH, temperature, salinity, alkalinity and total carbon by using CO2SYS program

*Significantly different than 400 µatm, † significantly different than 2000 µatm

[a]Significantly different than 400 µatm, [b]significantly different than 2000 µatm

Table 2 MS/MS identification of the protein spots of sea urchin tube feet that showed constant (a-d) or significantly different volumes (1-8) in response to elevated CO_2 conditions

Spot No.	Protein name	Species	Accession no (NCBI)	Theoretical mass (kDa)/pI	Observed mass (kDa)/pI	Fold 10000µatm/400µatm
Constant proteins						
a	Actin-1	*Strongylocentrotus purpuratus*	ACTA_STRPU	41.8/5.3	39.0/5.7	NA
b	Tropomyosin	*Paracentrotus lividus*	AM197503	32.7/4.7	34.7/4.7	NA
c	Voltage-dependent anion channel 2	*Paracentrotus lividus*	AM187061	31.1/8.8	29.4/7.2	NA
d	Calmodulin-A	*Strongylocentrotus intermedius*	CALM_STRIE	17.6/4.1	18.9/3.8	NA
Differentially accumulated proteins						
1	NF					+1.5
2	Tubulin beta chain	*Paracentrotus lividus*	TBB_PARLI	50.1/4.7	47.9/5.2	+1.4
3	Tropomyosin fragment	*Paracentrotus lividus*	AM197503	32.7/4.7	28.3/5.0	+1.5
4	Actin N-terminal fragment	*Strongylocentrotus purpuratus*	ACTA_STRPU	41.8/5.3	25.4/5.1	+1.4
5	NF					+1.4
6	NF					+1.6
7	Myosin light chain	*Paracentrotus lividus*	AM573676	17.0/4.8	17.4/5.3	-1.7
8	Actin C-terminal fragment	*Strongylocentrotus purpuratus*	ACTA_STRPU	41.8/5.3	17.4/6.8	-1.5

NF = Not found
NA = Not available

Figure S1. Magnified images of protein spots that showed significantly different changes in sea urchin tube feet between 400 µatm, 2000 µatm and 10000 µatm treatment (Mean ±SD; $P < 0.05$).

Spot No. 1

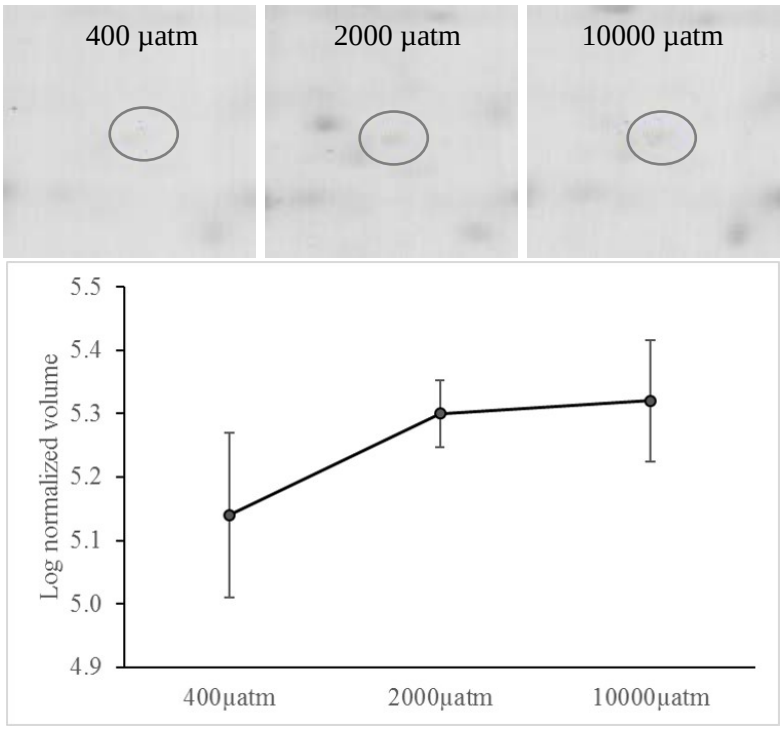

Spot No.2

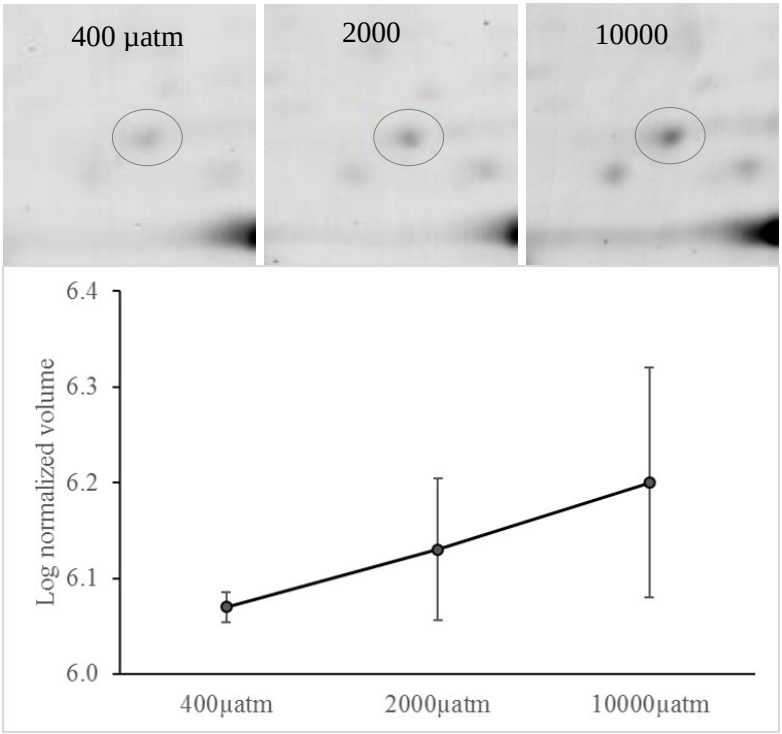

Spot No.3

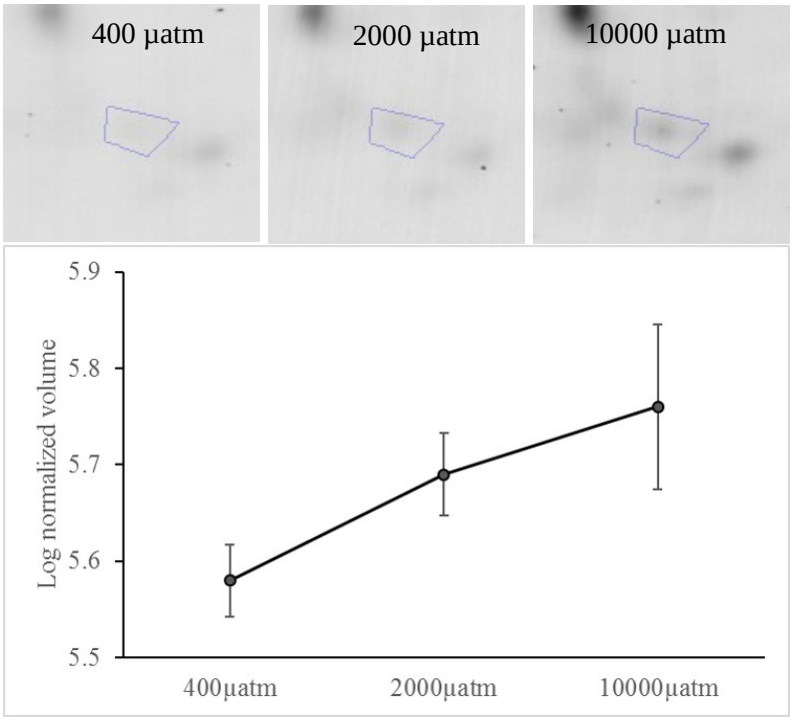

Spot No.4

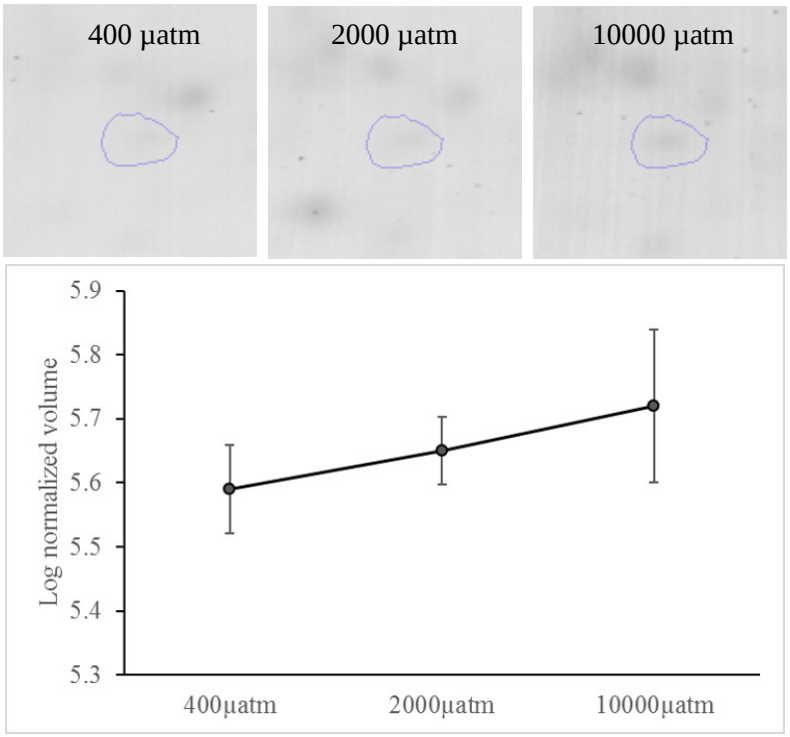

Spot No.5

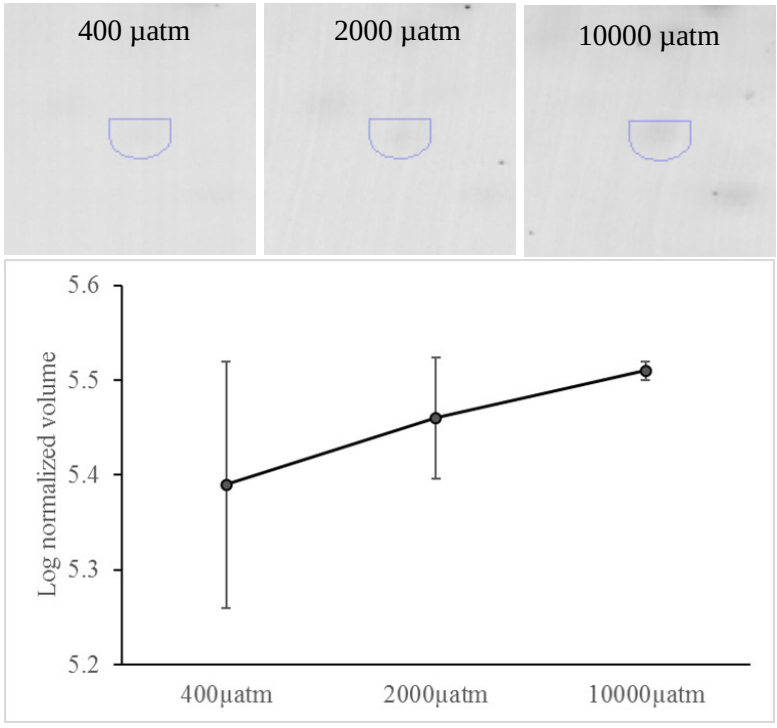

Spot No.6

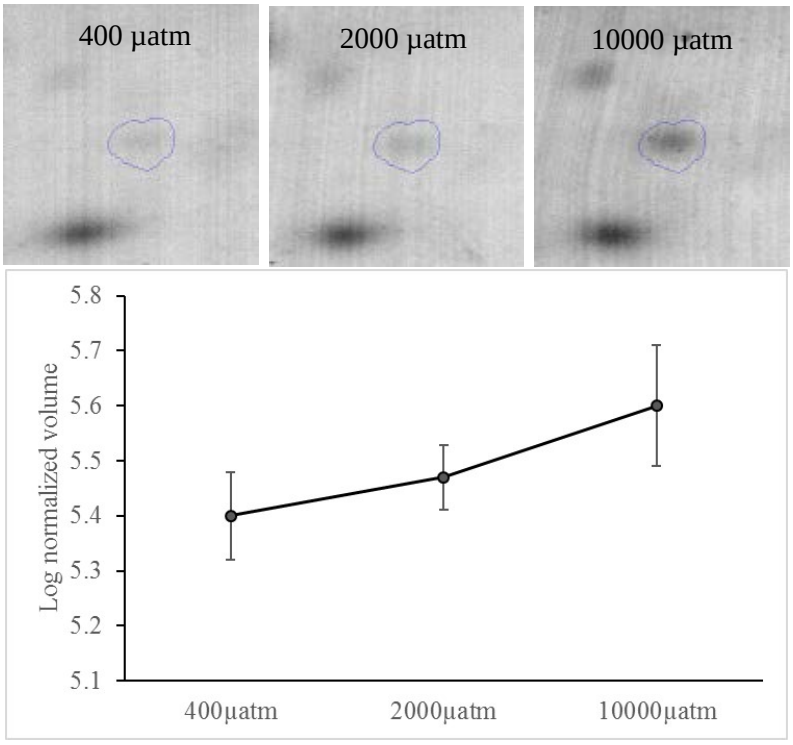

Spot No.7

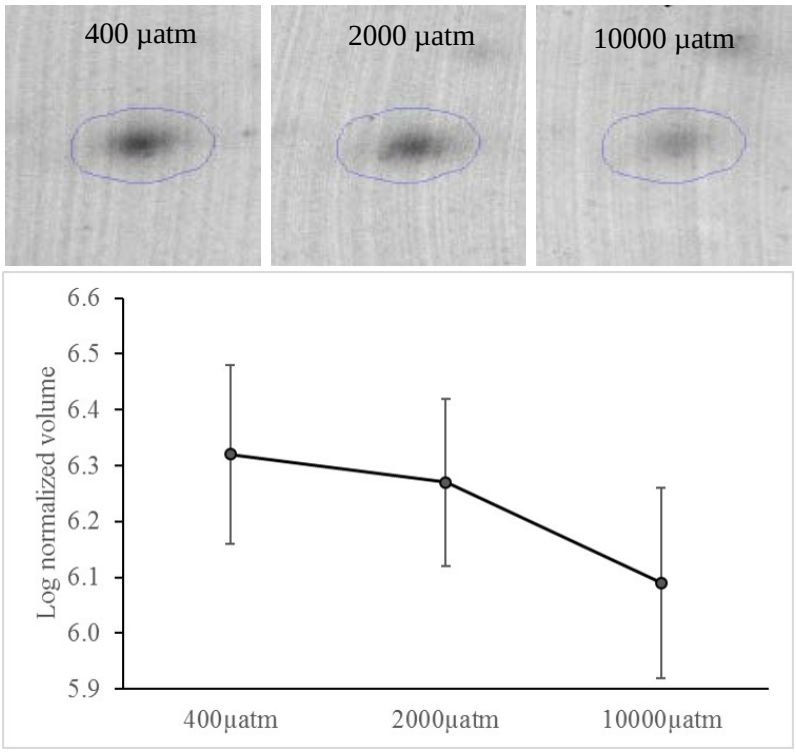

Spot No.8

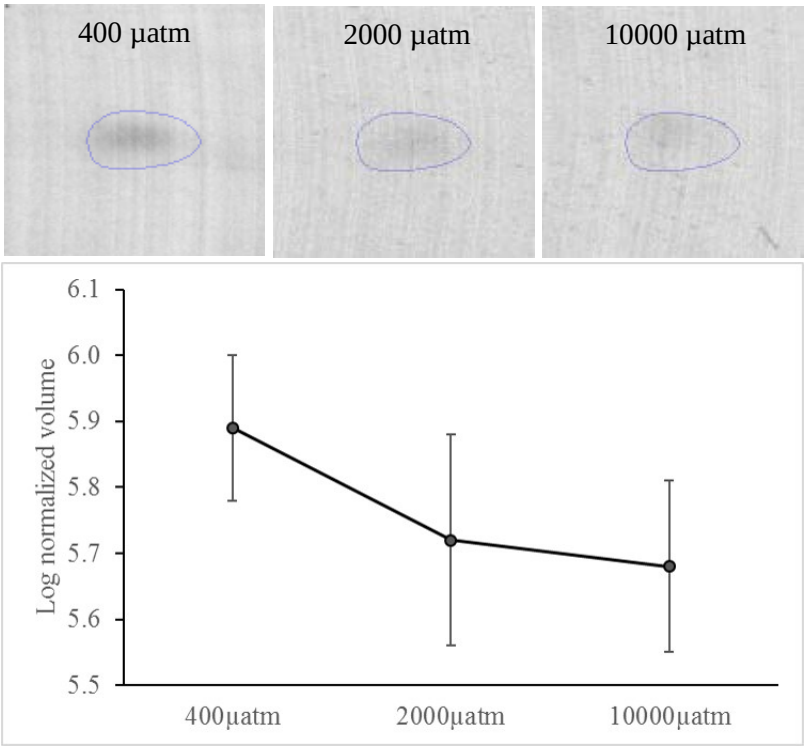

Figure S2 Full peptide sequence of actin of sea urchin *Pseudocentrotus depressus*: Bold texts are peptide sequence of actin N-terminal fragment (up) and actin C-terminal (down). Highlight is amino acid sequence around the caspase-cleaved site and closed arrow is the site of cleavage by caspase.

MCDEEVAALVVDNGSGMCKAGFAGDDAPRAIFPSIVGRPRHQGVMVGMGQKDS
YVGDEAQSKRGILTLKYPIEHGIVTNWDDMEKIWHHTFYNELR**VAPEEHPVLLT**
EAPLNPKANREKMTQIMFETFNTPAMYVAIQAVLSLYASGRTTGIVMDTGDGVTH
TVPIYEGYALPHAILRLDLAGRDLTDYLMKILTERGYSFTTTAEREIVRDIKEKLCY
VALDFEQEMATAASSSSLEKSYELPDGQVITIGNERFRCPEALFQPAFLGMESPGIH
ETTYNSIMKCDIDIRKDLYANTVLSGGTSMYPGIADRMQKEITSLAPSTMKIKIIAP
PERKYSVWIGGSILASLSTFQQMWISK**QEYDESGPSIVHR**KCF

Table S1 Contraction force of tube feet in individual sea urchin and statistics analysis

Sea urchin No.	Contraction force (Newton)								
	400 µatm			2000 µatm			10000 µatm		
	1	2	3	1	2	3	1	2	3
1	0.0451	0.0569	0.0332	0.0114	0.0164	0.0212	0.0012	0.0051	0.0028
2	0.0259	0.0577	0.0644	0.0314	0.0189	0.0140	0.0049	0.0072	0.0062
3	0.0550	0.0393	0.0192	0.0347	0.0180	0.0359	0.0226	0.0291	0.0029
4	0.0442	0.0373	0.0209	0.0312	0.0383	0.0283	0.0336	0.0226	0.0229
5	0.0228	0.0285		0.0199	0.0331	0.0324	0.0015	0.0012	0.0002
6	0.0192	0.0671		0.0412			0.0091	0.0061	0.0021
7	0.0320	0.0438		0.000			0.0122	0.0048	

One-way ANOVA

	Sum of Squares	df	Mean Square	F	P
Between groups	0.003	2	0.001	13.885	0.000
Within groups	0.002	18	0.000		
Total	0.005	20			

Multiple comparisons (Tukey HSD)

(I)Treatment	(J)Treatment	Mean difference (I-J)	Std. Error	P
1	2	0.01478	0.00553	0.039
	3	0.02915	0.00553	0.000
2	1	-0.01478	0.00553	0.039
	3	0.01437	0.00553	0.046
3	1	-0.02915	0.00553	0.000
	2	-0.01437	0.00553	0.046

Treatment 1 = 400 µatm, Treatment 2 = 2000 µatm, Treatment 3 = 10000 µatm

Table S2 Results of MS/MS ion search and BLAST search for protein identification

Spot No	Protein ID	EST (Accession No.)	Homolog (Accession No.)	Species	m/z	Sequence	Delta	Miss	Score	Expect
Constant proteins										
a	Actin-1	ND	ACTA_STRPU	*Strongylocentrotus purpuratus*	1790.12 1954.31	SYELPDGQVITIGNER VAPEEHPVLLTEAPLNPK	0.19 0.25	1 0	83 42	5.1e-006 0.024
b	Tropomyosin	gi|89438467	AM197503	*Paracentrotus lividus*	1686.96 1762.12	RLETIEVEADENLR KLQMTEQQLEVAEAK+oxidation	0.10 0.21	1 1	92 39	7.8e-007 0.11
c	Voltage dependant anion channel 2	gi|89444236	AM187061	*Paracentrotus lividus*	2531.16	TADFQLHTAVNEGSDFSGSIYQK +oxidation	-0.01	0	68	0.0001
d	Calmodulin-A	ND	CALM_STRIE	*Strongylocentrotus intermedius*	1738.68	VFDKDGNGFISAAELR	-0.2	1	77	1.9e-005
Differentially accumulated proteins										
1	NF									
2	Tubulin beta chain	ND	TBB_PARLI	*Paracentrotus lividus*	1159.61 1636.67 1959.00	LAVNMVPFPR+oxidation LHFFMPGFAPLTSR+oxidation GHYTEGAELVDSVLDVVR	-0.02 -0.16 0.02	0 0 0	52 42 60	0.0074 0.059 0.00096
3	Tropomyosin fragment	gi|89438467	AM197503	*Paracentrotus lividus*	1686.88 1761.94	RLETIEVEADENLR KLQMTEQQLEVAEAK + oxidation	0.01 0.03	1 1	63 51	0.0006 0.01
4	Actin N-terminal fragment	ND	ACTA_STRPU	*Strongylocentrotus purpuratus*	1954.18	VAPEEHPVLLTEAPLNPK	0.11	0	72	5.4e-005
5	NF									
6	NF									
7	Myosin	gi|139327852	AM573676	*Paracentrotus lividus*	1011.70 1271.72	HVLSTLGER LEEAEVDIIIK	0.14 0.01	0 0	43 45	0.08 0.05
8	Actin C-terminal fragment	ND	ACTA_STRPU	*Strongylocentrotus purpuratus*	1516.69 1790.91	QEYDESGPSIVHR SYELPDGQVITIGNER	-0.01 0.02	0 0	43 67	0.059 0.00031